Rough Set Based Modeling and Visualization of the Acoustic Field Around the Human Head

Piotr Szczuko(✉), Bożena Kostek, Józef Kotus, and Andrzej Czyżewski

Faculty of Electronics, Telecommunications and Informatics, Multimedia Systems Department and Audio Acoustics Laboratory, Gdańsk University of Technology, Narutowicza 11/12, 80-233 Gdańsk, Poland
{szczuko,kostek,joseph,andcz}@sound.eti.pg.gda.pl

Abstract. The presented research aims at modeling acoustical wave propagation phenomena by applying rough set theory in a novel manner. In a typical listening environment sound intensity is determined by numerous factors: a distance from a sound source, signal levels and frequencies, obstacles' locations and sizes. Contrarily, a free-field is characterized by direct, unimpeded propagation of the acoustical waves. The proposed approach is focused on processing sound field measurements performed in an anechoic chamber, collected by a dedicated acoustic probe, comprising thousands of datapoints for six signal frequencies, with and without the presence of a dummy head in a free-field. The rough set theory is applied for modeling the influence of an obstacle that a dummy head creates in a free-field and the effects of the head acoustic interferences, shading and diffraction. A data pre-processing method is proposed, involving coordinate system transformation, data discretization, and classification. Four rule sets are acquired, and achieved accuracy and coverage are assessed. Final results allow simplification of the model and new method for visualization.

Keywords: Rough sets · Imprecision · Acoustical field visualization

1 Introduction

It is important to emphasize that, in general, analytic models as well as acoustic field measurements provide useful information about pressure acoustics, pressure fields, but none currently offers a full vector mapping of the acoustic energy flow in front of and behind obstacles. Interference, diffraction, and scattering of waves make the real field very complex and challenging in terms of creating truly faithful theoretical frameworks. Taking these facts into consideration, the authors decided to conduct measurements of the vector acoustic field around a so-called dummy head imitating human head, using the sound intensity technique [4] and to enable resulting data processing employing a soft computing approach originating from the rough set methodology [13].

M. Kryszkiewicz et al. (Eds.): PReMI 2015, LNCS 9124, pp. 418–427, 2015.
DOI: 10.1007/978-3-319-19941-2_40

2 Measurement Methodology

Measurements were carried out in an anechoic chamber which is characterized by the free-field conditions, to avoid the problem of reflections coming from walls and obstacles. The acoustic intensity distribution was obtained using a sound intensity measurement technique, namely a 3D Acoustic Vector Sensor (AVS) [2, 5, 8–10, 14] was employed. AVS measures the acoustic particle velocity directly, instead of a sound pressure, which is captured by conventional microphones [6, 16]. The AVS senses air flow across two resistive strips of platinum that are heated up to approximately 200°C to provide temperature difference being the result of cooling by air flow [3]. The sensor itself is very miniature: typical dimensions of the wires are 5 μm in diameter and 1 to 3 mm in length, thus giving a nearly pin-point measurement, at the same time not causing the acoustic field disturbance. It operates in a flow range of 10 nm/s up to about 1 m/s. Each sensor is sensitive in only one direction, therefore, three orthogonally placed transducers are used. In combination with pressure measurement by a microphone, the sound field in a single point is fully characterized, and the acoustic intensity vector, which is the product of pressure and particle velocity, can be determined. This intensity vector indicates the acoustic energy flow.

Sound intensity is the average rate at which sound energy is transmitted through the unit area perpendicular to the specified direction at the considered point. The intensity in a certain direction is the product of sound pressure (scalar) p(t) and the particle velocity (vector) component in that direction u(t). The time-averaged intensity I in a single direction is given by (1) [4]:

$$I = \frac{1}{T} \int_T p(t)u(t)dt \tag{1}$$

In the applied algorithm of sound intensity calculation, the averaging time T was 4096 samples (with the sampling frequency of 48 kHz). It means that the measured value was updated more than 10 times per second. A single intensity measurement takes 1 s, being an average of values.

Using the AVS, the particular sound intensity components can be obtained based on Eq. (1). The sound intensity vector in three dimensions is composed of the acoustic intensities in three orthogonal directions (x, y, z) (2):

$$\vec{I} = I_x\vec{e}_x + I_y\vec{e}_y + I_z\vec{e}_z \tag{2}$$

Sound intensity calculation can be performed in the time domain or in the frequency domain [8, 9]. Due to the fact that the multi-harmonic signal was employed in the measurements, a method for calculating the sound intensity in the frequency domain was applied for this purpose. The detailed information about algorithm and methodology of the measurement performed can be found in [10].

The full three dimensional sound intensity vector field can be determined within the audible frequency range from 20 Hz up to 20 kHz [2, 14]. As an example of the measurement results, Fig. 1 shows sound intensity distribution characteristics for 1000 Hz.

The signal was radiated from the center loudspeaker in a 5.1 surround sound setup (top-middle of images), without and with a dummy head present in the field, and additionally a difference between these two measurements is visualized. The wave phenomena such as diffraction and interference are clearly visible. It is also easy to observe local compression of sound energy (in front of and behind the head), as well as the increase of the intensity level on both sides of the head.

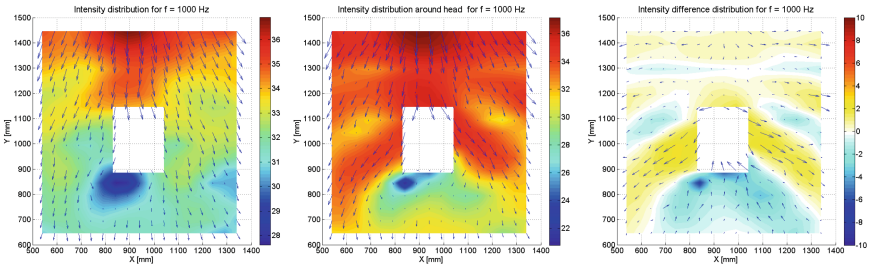

Fig. 1. Sound intensity distribution for 1000 Hz, signal from the center loudspeaker. From left: free-field and no dummy head; dummy head present in the field; the difference expressing influence of the head

The research presented in this paper shows an attempt to model acoustical wave propagation phenomena by applying rough set theory to acoustic field visualization. The approach proposed is focused on processing sound field measurement performed in an anechoic chamber, collected by a dedicated acoustic probe. Datapoints for six signal frequencies with and without the presence of a dummy head in a free-field, resulted from the measurements, are analyzed employing the rough set theory. However, first, a data pre-processing method, involving coordinate transformation is proposed. Also, data discretization for modeling the influence of an obstacle that a dummy head creates in a free-field [7] is performed before the rough set-based analysis. In consequence, a rule set is acquired, allowing for the model simplification and visualization.

3 Acoustic Field Parameterization

The acoustic field was measured by a vector sensor, capable of registering values of particle velocity flow in x, y, z directions. This sensor was positioned precisely in given coordinates by a dedicated Cartesian robot arm [11]. As a result the sound intensity at a certain point in space has been obtained.

Measurements were conducted in two conditions: (1) with the speaker emitting test signals in an anechoic chamber environment; (2) the same speaker and signals emitted but along with a dummy head, positioned in the center of the measured space. Collected measurement results enabled to visualize directional characteristic of the speaker and open-space sound propagation phenomena [12], on one hand; and impact of the head on sound propagation, compression and rarefaction on the other hand [15] (Fig. 2).

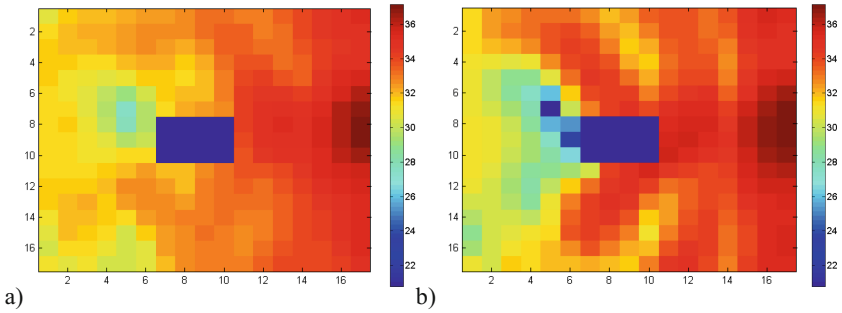

Fig. 2. Results of acoustic field measurements for 1000 Hz test signal: (a) field without the head, (b) field with the head

Measurements covered horizontal grid of 17 × 17 points, spaced evenly in interval of 50 mm, positioned at the level of ears of the dummy head.

3.1 Vector Field Data Preprocessing

The Cartesian coordinate system is convenient for positioning the robot arm and uniformly covering large spaces. Nevertheless, for further processing polar coordinates are to be used. A conversion from Cartesian to polar systems was made, assuming that the center of polar system is the head center, and direction 0 degrees is in front of it, the same as the speaker direction. For polar representation of acoustic field it was assumed that it is sufficient to analyze only 20 different directions (360 deg split into 18 degree wide slices), and 20 grades of distance from the center (Fig. 3), resulting in a discretization of the measured space.

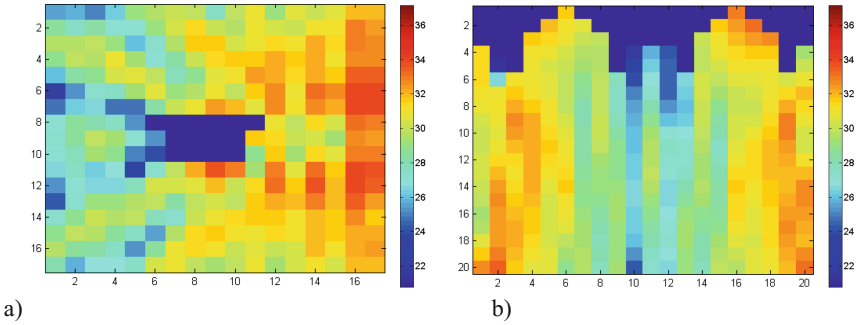

Fig. 3. Conversion of coordinates: (a) acoustic field with head present for 2000 Hz the Cartesian coordinate system, (b) in polar coordinates

For particular frequency of emitted sound, two measurements are available – empty space $I_{env}(x,y)$ and with the dummy head $I_{w\_head}(x,y)$ for every point in the space. A difference between these two reflects the influence of the head presence on sound propagation (see Fig. 4 and Eq. (3)).

$$I_{env} - I_{w\_head} = I_{influence} \tag{3}$$

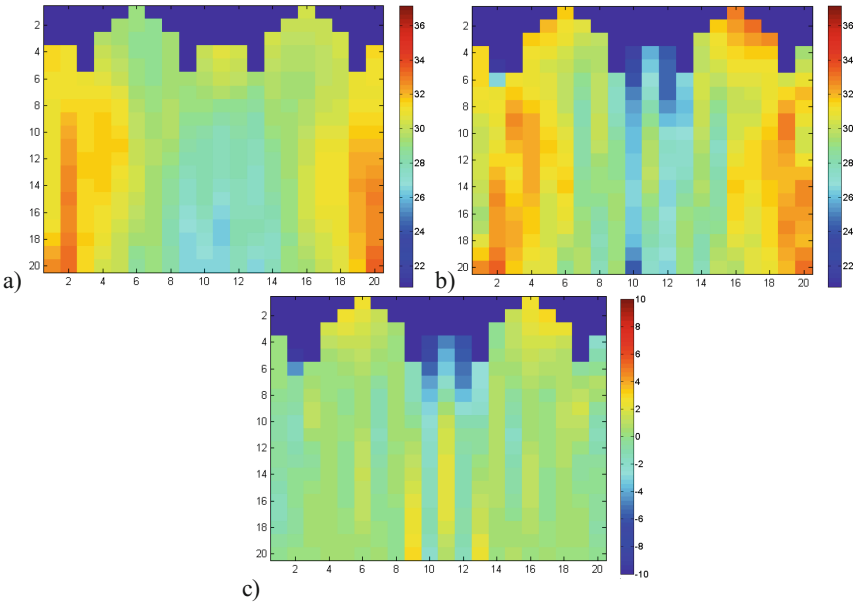

Fig. 4. Influence of head on sound propagation: (a) acoustic field for 2000 Hz in an empty space, (b) field with the head present, (c) difference reflecting the influence

It is assumed, that in different conditions the factor I_{env}, reflecting the propagation in the environment and the speaker characteristics, would be different. The presence of the head in such a new condition would also result in different values of I_{w_head}. Nevertheless the $I_{influence}$ should remain unchanged, as long as the head position its size, and its relative position to the speaker is unchanged. Therefore, the focus is on the analysis of the head influence only, expressed as above.

Due to the nature of a sound wave, the measurement is not precise. Non-uniform propagation from the not ideal speaker[1] and numerous reflections from the head, result in wave interferences, that are not observed accurately, as measurements are taken only in selected points in space. Therefore, single measurement reflects only roughly the sound intensity at a certain point. It should be recalled here that wave interference is the interaction of two sound waves traveling in the same medium. The interference of waves causes the shape of the pressure wave to combine in the medium into a complex waveform. If the *compressions* of two similar sounds meet, they will combine and have twice the amplitude. If two *rarefaction* sections intersect, they will combine in the medium and a *rarefaction* of twice the amplitude will result [17].

[1] The ideal sound source is a point emitting in all directions with the same level.

Due to the low precision of measured values, it is advisable to introduce a general and rough representation of the sound intensity. Thus, a discretization of measurements was performed, focused on forming classes reflecting the sound intensity changes, i.e. (1) high *rarefaction*, (2) medium *rarefaction*, (3) unchanged, (4) medium *compression*, (5) high *compression* (Fig. 5).

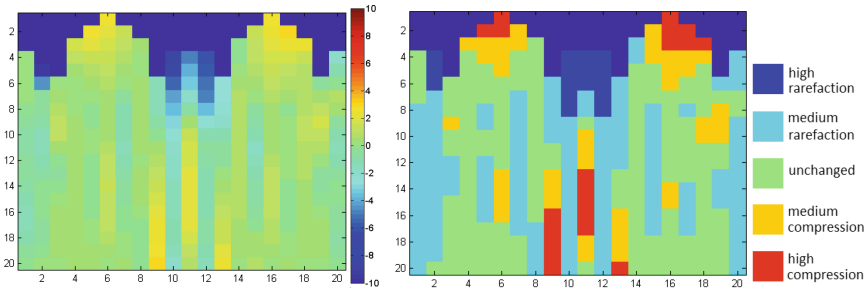

a) b)

Fig. 5. Sound intensity changes for 2000 Hz: (a) original values, (b) discretized into five classes

The discretization is based on the expert knowledge: e.g. the intensity decrease of −3 dB or more is regarded as high *rarefaction*, a decrease in range of (−3 dB, 0 dB) is not significant, therefore regarded as medium *rarefaction*, an increase in intensity level by 1 dB can be either measurement error or the result of a minor interference, therefore is medium *compression*, and finally, an increase larger than +2 dB is a major interference, and is high *compression* (Table 1).

Table 1. Discretization of sound intensity values

Range of values	$I_{influence} \leq -3$	$-3 < I_{influence} < 0$	$0 \leq I_{influence} < 1$	$1 \leq I_{influence} < 2$	$I_{influence} \geq 2$
Assigned class	hraref.	mraref.	unch.	mcomp.	hcomp.

Class names:
hraref. - high rarefaction
mraref. - medium rarefaction
unch. - unchanged
mcompr.- medium compression
hcompr. - high compression

As a result of the described preprocessing, the input data from sound level measurements are discretized in terms of direction (20 angles), distance (20 grades), and value (5 classes).

3.2 Rough Set Based Reasoning

A decision table containing four discrete attributes from all measurements was created: angle, distance, frequency, $I_{influence}$, the last one treated as the decision attribute. 400 points were provided for six frequencies of: 250 Hz, 500 Hz, 1000 Hz, 2000 Hz, 4000 Hz, and 8000 Hz, resulting in 2400 objects in the table (Fig. 6). The table was processed in the RSES Rough Set Exploration System [1]. An exhaustive algorithm was used for determining the reduct, and it comprised all three attributes (angle, distance, frequency).

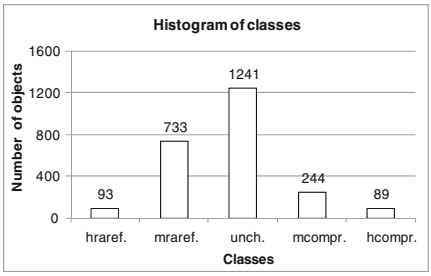

Fig. 6. Histogram of classes in the 2400 objects decision table

Analyzing all objects in the table, a set of rules was derived, resulting in 2034 rules: 97 % of rules included three attributes, and 3 % only two attributes. Mean support was equal to 1.2.

The next step was generalization of rules, with a factor of 0.9. This resulted in the same number of rules, but with greatly increased mean support, equal to 57.3. One of the rules with the highest support of 180 objects, is related to region of unchanged intensity region, present in almost all frequencies (4):

$$\begin{aligned} &\text{IF } (\text{angle} = \{1 \text{ or } 2 \text{ or } 3\}) \\ &\text{AND } (\text{dist} = \{1\text{or } 2 \text{ or } 3 \text{ or } 9 \text{ or } 10 \text{ or } 11 \text{ or } 12 \text{ or } 13 \text{ or } 19 \text{ or } 20\}) \\ &\text{THEN } \left(\text{value} = \{''\text{unch.}''\}\right) \end{aligned} \tag{4}$$

Over 2000 rules explaining relations observed in a database of 2400 objects is definitely too high number, close to overfitting. Therefore a series of experiments were performed, testing accuracy of classification with reduced rule sets.

4 Experiments and Results

Rules with the lowest support were removed, using three thresholds (minimal support of 3, 10 and 20), and classification tests were performed on the decision table with all 2400 objects. A comparison of performance reveals that satisfactory level of generalization was obtained, as reduction of number of rules to 29 % of initial number still yields high accuracy and coverage (Table 2) (Fig. 7).

Table 2. Comparison of initial and filtered rule sets: support, number of rules and achieved accuracy and coverage

	Rule sets			
	Initial set	Filtered A	Filtered B	Filtered C
Minimal support of rules	1	3	10	20
Maximal support of rules	20	194	194	194
Mean support of rules	1.2	50.1	60.4	69.9
Number of rules (percent of initial set)	2034 (100 %)	588 (29 %)	476 (23 %)	396 (19 %)
Accuracy	0.95	0.937	0.916	0.885
Coverage	1.0	0.999	0.936	0.854

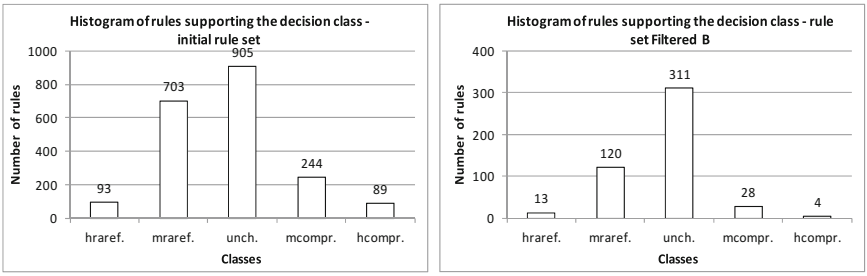

Fig. 7. Number of rules supporting decision classes in initial rule set and Filtered B set

Detailed results of classification of all objects using 588 rules (rule set "Filtered A") reveal confusion between medium rarefaction/compression/unchanged cases, where the observed value of the sound intensity change varies by ± 1 dB, and can be explained by the measurement imprecision. Adequate high accuracy and coverage are achieved (Table 3). Reduction of rules to 476 (rule set "Filtered B") shows a significant loss of coverage, especially for high compression cases, and the total performance is questionable (Table 4).

Summarizing, the resulted 588 "Filtered A" rule set, is a good compromise between accuracy and the ability to describe dependencies of angle, distance, frequency, and result compression/rarefaction in the sound field. Confusion between medium changes of ± 1 dB is negligible, by means of perception of the sound by the human ear.

Table 3. Summary of results for rules with minimal support of 3

		Predicted class							
		un-changed.	med. compr.	med. rare-faction	high compr.	high rare-faction	No. of obj.	Accu-racy	Cov-erage
Actual class	unchanged	**1,224**	1	16	0	0	1,241	0.986	1
	med. compr.	16	**228**	0	0	0	244	0.934	1
	med. rarefaction	108	0	**624**	0	1	733	0.851	1
	high compr.	0	0	0	**87**	0	89	1	0.978
	high rarefaction	1	0	7	0	**85**	93	0.914	1
	True positive rate	0.91	1	0.96	1	0.99			

Table 4. Summary of results for rules with minimal support of 10

		Predicted class							
		un-changed.	med. compr.	med. rare-faction	high compr.	high rare-faction	No. of obj.	Accu-racy	Cov-erage
Actual class	unchanged	**1,224**	1	16	0	0	1,241	0.986	1
	med. compr.	48	**124**	2	0	0	244	0.713	0.713
	med. rarefaction	109	0	**607**	0	1	733	0.847	0.978
	high compr.	2	0	0	**24**	0	89	0.923	0.292
	high rarefaction	1	0	8	0	**80**	93	0.899	0.957
	True positive rate	0.88	0.99	0.96	1	0.99			

Accuracy: TP/(TP + FN), e.g. 24/(24 + 2) = 0.923 for high compression.
Coverage: (TP + FN)/(No. of obj.), e.g. (24 + 2)/89 = 0.292 for high compression.
True positive rate: TP/(TP + FP), e.g. 607/(16 + 2+607 + 8) = 0.96 for med. rarefaction.

5 Conclusions

A novel approach to modeling and visualization of the sound field was proposed in the paper employing the rough set-based mechanism for the delivery of a rule set helping to study acoustical phenomena. The overall image of the acoustic field resulted from measurement comprises the effect of the obstacles appearing in a source radiation path, as well as the influence of scattered reflections together with their phase and amplitude relationship. The aforementioned measurements employed an acoustic intensity probe. The observation of acoustic wave distribution around the human head illustrates that phenomena occurring in the real acoustic field are more complex than those typically shown in acoustic field simulations. The wave phenomena such as diffraction and additional interferences are clearly visible. The experiments conducted helped to verify the method for reducing the complexity of data resulted from acoustic field measurements.

Acknowledgements. The project was funded by the National Science Centre allocated on the basis of the decision DEC-2012/05/B/ST7/02151.

References

1. Bazan, J., Szczuka, M.S., Wróblewski, J.: A new version of rough set exploration system. In: Alpigini, J.J., Peters, J.F., Skowron, A., Zhong, N. (eds.) RSCTC 2002. LNCS (LNAI), vol. 2475, pp. 397–404. Springer, Heidelberg (2002)
2. de Bree, H.-E.: The microflown: an acoustic particle velocity sensor. Acoust. Aust. **31**(3), 91–94 (2003)
3. Cengarle, G., Mateos, T.: Comparison of Anemometric Probe and Tetrahedral Microphones for Sound Intensity Measurements. AES 130th Convention, Paper No. 8363, London, UK, 13–16 May 2011
4. Fahy, F.J.: Sound Intensity. Elsevier Applied Science, London (1989)
5. Jacobsen, F.: Sound intensity and its measurement and applications. Acoustic Technology, Department of Electrical Engineering Technical University of Denmark (2011)
6. Jacobsen, F., de Bree, H.-E.: Measurement of sound intensity: p-u probes versus p-p probes. In: Proceedings of NOVEM (2005)
7. Kahana, Y.: Numerical modelling of the head-related transfer function. Ph.D. Thesis, University of Southampton, UK (2000)
8. Kotus, J.: Application of passive acoustic radar to automatic localization, tracking and classification of sound sources. Inf. Technol. **18**, 111–116 (2010)
9. Kotus, J.: Multiple sound sources localization in free field using acoustic vector sensor. Multimedia Tools Appl., June 2013. doi:10.1007/s11042-013-1549-y
10. Kotus, J., Kostek, B.: Measurements and visualization of sound intensity around the human head in free field using acoustic vector sensor. J. Audio Eng. Soc. **63**(1/2), 99–109 (2015). doi:http://dx.doi.org/10.17743/jaes.2015.0009
11. Kotus, J., Plewa, M., Kostek, B.: Measurements and visualization of sound intensity around the human head using acoustic vector sensor. e-Brief 154, 136th AES Convention, April 26–29 Berlin, Germany (2014)
12. Merimaa, J., Lokki, T., Peltonen, T., Karjalainen, M.: Measurement, Analysis, and Visualization of Directional Room Responses. 111 AES Convention, New York, USA (2001)
13. Pawlak, Z.: Rough sets. Int. J. Comput. Inform. Sci. **11**(5), 341–356 (1982)
14. Raangs, R., Druyvesteyn, W.F., de Bree, H.E.: A low cost Intensity Probe. 110 AES Convention, Paper no. 5292, Amsterdam (2001)
15. Weyna, S.: Identification of reflection and scattering effects in real acoustic flow field. Arch. Acoust. **28**(3), 191–203 (2003)
16. Woszczyk, W., Iwaki, M., Sugimoto, T., Ono, K., de Bree, H.-E.: Anechoic Measurements of Particle-Velocity Probes Compared to Pressure Gradient and Pressure Microphones. 122 AES Convention: May 2007, Paper Number: 7107 (2007)
17. Sound interference explanation. http://www.sound-physics.com/Sound/Interference/